PHYSICAL REVIEW D **92,** 014020 (2015)

Nature of $X(4260)$

L. Y. Dai,[1,*] Meng Shi,[1] Guang-Yi Tang,[1] and H. Q. Zheng[1,2,†]

[1]*Department of Physics and State Key Laboratory of Nuclear Physics and Technology, Peking University, Beijing 100871, Peoples Republic of China*

[2]*Collaborative Innovation Center of Quantum Matter, Beijing 100871, Peoples Republic of China*

(Received 16 March 2015; published 16 July 2015)

We study the properties of the $X(4260)$ resonance by reanalyzing all experimental data available, especially the $e^+e^- \to J/\psi\pi^+\pi^-$, $\omega\chi_{c0}$ cross section data. The final-state interactions of the $\pi\pi$, $K\bar{K}$ coupled-channel system are also taken into account. A sizable coupling between $X(4260)$ and $\omega\chi_{c0}$ is found. The inclusion of the $\omega\chi_{c0}$ data indicates a small value of $\Gamma_{e^+e^-} = 23.30 \pm 3.55$ eV.

DOI: 10.1103/PhysRevD.92.014020 PACS numbers: 14.40.Pq, 14.40.Rt

I. INTRODUCTION

The $X(4260)$ resonance [previously called $Y(4260)$] was found by the *BABAR* Collaboration in the initial-state radiation process $e^+e^- \to \gamma_{\rm ISR}J/\psi\pi^+\pi^-$ in 2005 [1], and was later confirmed by the CLEO [2] and Belle [3] collaborations. In Ref. [4], the mass and width of this resonance were given as $M = 4251 \pm 9$ MeV and $\Gamma = 120 \pm 12$ MeV, respectively. Furthermore, $\Gamma_{ee} \times {\rm Br}(J/\psi\pi\pi) = 9.7 \pm 1.1$ eV [3] or 9.2 ± 1.5 eV [5]. From the theoretical viewpoint, the structure of $X(4260)$ is very interesting, since it is generally thought that there are not enough unassigned vector states in the charmonium spectrum [including the recently reported $Y(4360)$ and $X(4630)/Y(4660)$ states]. The masses are also inconsistent with naive quark-model predictions [6]; the only such 1^{--} states expected up to 4.4 GeV are 1S, 2S, 1D, 3S, 2D, and 4S, and they seem to be well established [7]. The situation is depicted in Fig. 1. It is noticed that above the $D\bar{D}$ threshold the number of 1^{--} states given by the quark-model prediction is inconsistent with that given by experiments. One tends to believe that the discrepancy between the naive quark-model prediction and the observed spectrum is ascribed, at least partially, to the existence of many open charm thresholds, since the latter will distort the spectrum. The situation is depicted in Fig. 2. Because of the situation described, above many theoretical papers have been devoted to the investigation of $X(4260)$. In the literature, many models have been made, e.g., the $\chi_{c0}\rho^0$ molecule [8], $\omega\chi_{c1}$ molecule [9], $c\bar{c}g$ hybrid state [10–14], $\Lambda_c\bar{\Lambda}_c$ baryonium [15], $D_1\bar{D}$ or $D_0\bar{D}_0^*$ molecule [16–18], hadro-charmonium [19], the nonresonant explanation [20,21], etc. Besides, the tetraquark-state explanation is also very interesting [22–28], especially after the two resonances $Z_c(3900)$ and $Z_c(4025)$ were recently found in the $J/\psi\pi$ and $D^{(*)}\bar{D}^{(*)}$ channels in e^+e^- annihilation near 4.26 GeV by the BESIII Collaboration [29], and confirmed by the Belle [30] and CLEO [31] collaborations. However, the open charm channels (such as $\bar{D}D^*$, $D\bar{D}^*$, and $D^*\bar{D}^*$) are not found in the final states of $X(4260)$ decays [32–34], making the properties of $X(4260)$ even more mysterious.

The present authors have also studied the $X(4260)$ issue in a previous edition of the present paper ([35], hereafter denoted as V1). Through a careful comparison with available experimental data, it was found that $X(4260)$ has a sizable coupling to the $\omega\chi_{c0}$ channel, but not to other (nearby) channels. Inspired by our result, a recent experimental analysis [36,37] showed that there is indeed a sizable $\omega\chi_{c0}$ final-state signal in e^+e^- collisions at around 4.26 GeV, which hints that $X(4260)$ may have a large coupling to $\omega\chi_{c0}$, although it is not totally clear whether the $\omega\chi_{c0}$ is from the continuum spectrum or the $X(4260)$ resonance, or from both. Furthermore, the cross section of the $h_c\pi\pi$ channel [38] was also measured at this energy, implying that $X(4260)$ may also couple to it. Because of all of these new observations, we have an urge to upgrade the work of V1. In the present paper, we continue the preceding analysis by including the $\omega\chi_{c0}$ (and also $h_c\pi\pi$) cross-section data, and we find that the major qualitative conclusion of V1 still holds; that is, $X(4260)$ couples significantly to $\omega\chi_{c0}$ but not to other nearby thresholds. Furthermore, we find that the $X(4260)$ resonance is likely to maintain a small e^+e^- width, thanks to the new $\omega\chi_{c0}$ data.

The paper is organized as follows. In Sec. II we review the theoretical tools we use in this paper, where special emphasis is placed on the final-state interactions (FSI) between pions and kaons. In Sec. III we give a detailed description of our numerical fit program with two scenarios: one that does not include the $\omega\chi_{c0}$ cross-section data [36,37], and on that does. Both of them take into account the effect of the possible $h_c\pi\pi$ decay channel. The pole locations of the $X(4260)$ propagator are also investigated. Finally, conclusions and physical discussions of the present analysis are given in Sec. IV.

*Present address: Center for Exploration of Energy and Matter, 2401 Milo B. Sampson Lane, Bloomington, Indiana 47408, USA.

†zhenghq@pku.edu.cn

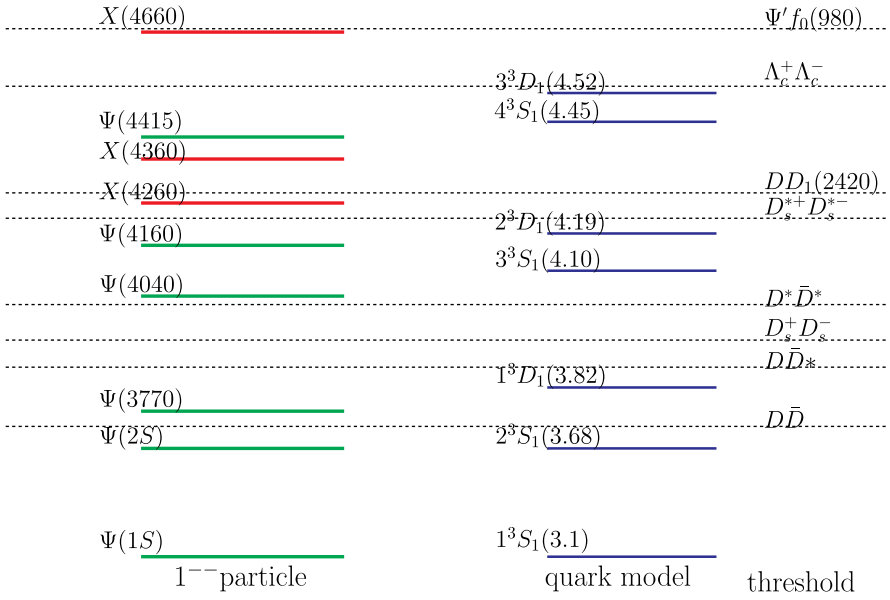

FIG. 1 (color online). $X(4260)$ and nearby resonances from the naive quark-model calculation [6].

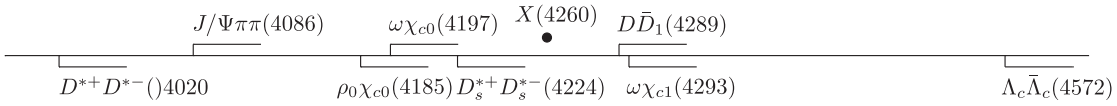

FIG. 2. Location of $X(4260)$ and nearby thresholds.

II. THEORETICAL DISCUSSIONS OF $e^+e^- \to J/\psi\pi\pi$

A. Effective Lagrangian describing $e^+e^- \to J/\psi\pi\pi$ interactions

Assuming that $X(4260)$ is a $J^{PC} = 1^{--}$ chiral singlet particle, there are two methods to describe the $J^{PC} = 1^{--}$ field: a vector and an antisymmetric tensor. The antisymmetric tensor representation of a massive vector field is equivalent to the vector representation [39] in the on-shell situation. However, the high-energy behavior of the tensor representation is better than the vector representation. [40] In the antisymmetric tensor representation, the equation of motion of a massive 1^{--} field $W^{\mu\nu}$ ($W^{\mu\nu} = -W^{\nu\mu}$) is

$$\partial^\mu\partial_\sigma W^{\sigma\nu} - \partial^\nu\partial_\sigma W^{\sigma\mu} + M^2 W^{\mu\nu} = 0. \tag{1}$$

The propagator is

$$\begin{aligned}&\langle 0|T\{W_{\mu\nu}(x)W_{\rho\sigma}(y)\}|0\rangle \\ &= iM^{-2}\int\frac{d^4k e^{-ik(x-y)}}{(2\pi)^4} \\ &\times\frac{g_{\mu\rho}g_{\nu\sigma}(M^2-k^2)+g_{\mu\rho}k_\nu k_\sigma - g_{\mu\sigma}k_{n\nu}k_\rho - (\mu\leftrightarrow\nu)}{M^2-k^2-i\epsilon}.\end{aligned} \tag{2}$$

This propagator corresponds to the normalization [39]

$$\langle 0|W_{\mu\nu}|W,p\rangle = iM^{-1}[p_\mu\epsilon_\nu(p) - p_\nu\epsilon_\mu(p)]. \tag{3}$$

The transition operator between a photon and $X(4260)$ in the antisymmetric representation is the following:

$$\mathcal{L}_{\gamma X} = g_0 X_{\mu\nu}F^{\mu\nu}, \tag{4}$$

where we use the antisymmetric representation $X_{\mu\nu}$ to describe the 1^{--} state $X(4260)$, and $F_{\mu\nu}$ denotes the photon field strength. Notice that in the present notation, one has

$$\Gamma_{e^+e^-} = \frac{4\alpha}{3}\frac{g_0^2}{M_X}, \tag{5}$$

where we have neglected the electron-positron masses. For $X(4260)$ decay, the following effective Lagrangian is used, which is accurate in the leading order in the expansion in terms of theπ momentum in the center-of-mass frame of $\pi\pi$ system:

$$\begin{aligned}\mathcal{L}_{X\psi PP} = {}& h_1 X_{\mu\nu}\psi^{\mu\nu}\langle u_\alpha u^\alpha\rangle + h_2 X_{\mu\nu}\psi^{\mu\nu}\langle\chi_+\rangle \\ &+ h_3 X_{\mu\alpha}\psi^{\mu\beta}\langle u_\beta u^\alpha\rangle,\end{aligned} \tag{6}$$

where the antisymmetric representation $\psi^{\mu\nu}$ describes J/ψ. Up to the $O(p_\pi^2)$ level, in Eq. (6) there exist only three independent interaction terms with the coefficients h_1, h_2, and h_3. Further, $u_\mu = i(u^+\partial_\mu u - u\partial_\mu u^+)$ and

$$u = \exp\left\{ i\frac{\Phi}{\sqrt{2}F_\pi} \right\} \tag{7}$$

is the parametrization of the pseudo-Goldstone octet:

$$\Phi = \begin{pmatrix} \frac{1}{\sqrt{2}}\pi^0 + \frac{1}{\sqrt{6}}\eta_8 & \pi^+ & K^+ \\ \pi^- & -\frac{1}{\sqrt{2}}\pi^0 + \frac{1}{\sqrt{6}}\eta_8 & K^0 \\ K^- & \bar{K}^0 & -\frac{2}{\sqrt{6}}\eta_8 \end{pmatrix}. \tag{8}$$

The chiral symmetry-breaking term with the coefficient h_2 in Eq. (6) reads

$$\begin{aligned} \chi_+ &= u^+\chi u^+ + u\chi^+ u, \\ \chi &= 2B_0 \mathrm{diag}(m_u, m_d, m_s). \end{aligned} \tag{9}$$

The parameters F_π and B_0 can be fixed phenomenologically: $F_\pi \approx 92.4\mathrm{MeV}$ and $\langle 0|\psi\bar{\psi}|0\rangle = -F^2B_0[1+O(m_q)]$. Equation (6) can also be rewritten in an explicit form,

$$\begin{aligned} \mathcal{L}_1 &= \frac{4h_1}{F_\pi^2} X_{\mu\nu}F^{\mu\nu}\left(\partial_\rho\pi^+\partial^\rho\pi^- + \frac{1}{2}\partial_\rho\pi^0\partial^\rho\pi^0 + \partial_\rho K^+\partial^\rho K^- \right. \\ &\quad \left. + \partial_\rho K^0\partial^\rho\bar{K}^0 + \frac{1}{2}\partial_\rho\eta\partial^\rho\eta \right), \\ \mathcal{L}_2 &= -\frac{4h_2}{F_\pi^2} X_{\mu\nu}F^{\mu\nu}\left(m_\pi^2\pi^+\pi^- + \frac{1}{2}m_\pi^2\pi^0\pi^0 + m_K^2K^+K^- \right. \\ &\quad \left. + m_K^2K^0\bar{K}^0 + \left(\frac{2}{3}m_K^2 - \frac{1}{6}m_\eta^2\right)\eta\eta \right), \\ \mathcal{L}_3 &= \frac{4h_3}{F_\pi^2} X_{\mu\alpha}F^{\mu\beta}\left(\frac{1}{2}\partial_\beta\pi^+\partial^\alpha\pi^- + \frac{1}{2}\partial_\beta\pi^-\partial^\alpha\pi^+ \right. \\ &\quad + \frac{1}{2}\partial_\beta\pi^0\partial^\alpha\pi^0 + \frac{1}{2}\partial_\beta K^+\partial^\alpha K^- + \frac{1}{2}\partial_\beta K^-\partial^\alpha K^+ \\ &\quad \left. + \frac{1}{2}\partial_\beta K^0\partial^\alpha\bar{K}^0 + \frac{1}{2}\partial_\beta\bar{K}^0\partial^\alpha K^0 + \frac{1}{2}\partial_\beta\eta^0\partial^\alpha\eta^0 \right). \end{aligned} \tag{10}$$

B. Kinematics and tree-level amplitudes

We denote the momenta of e^-, e^+, $X(4260)$, J/ψ, π^+, and π^- as q_1, q_2, q, l, q^+, and q^-, respectively (see Fig. 3). The polarization of J/ψ is represented as ϵ_ψ, and $k_\pm = q^+ \pm q^-$. Then one has the following relations:

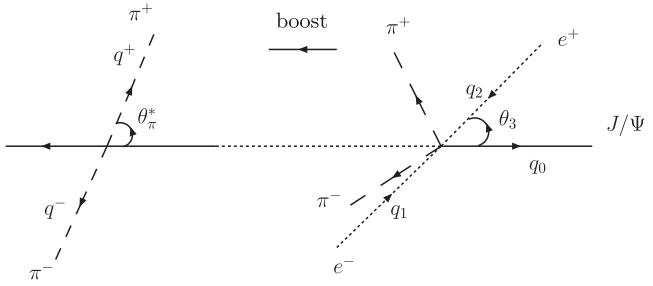

FIG. 3. A depiction of kinematics.

$$\begin{aligned} s &\equiv k_+^2, \\ k_-^2 &= -s\rho(s)^2 = 4m_\pi^2 - s, \\ l^2 &= M_{J/\psi}^2, \qquad k_+\cdot k_- = 0, \\ k_+\cdot l &= \frac{1}{2}(q^2 - M_{J/\psi}^2 - s), \end{aligned} \tag{11}$$

where $\rho(s) = \sqrt{1-\frac{4m_\pi^2}{s}}$. The amplitude of the $X \to J/\psi\pi^+\pi^-$ process at tree level is

$$\begin{aligned} i\mathcal{A}^{\mathrm{tree}} &= \frac{i4eg_0}{M_{J/\psi}F_\pi^2 q^2 D_X(q^2)}\bar{v}(q_1,s)\gamma_\lambda u(q_2,s') \\ &\quad \times\left\{ \left[4h_1\frac{1}{2}(s-2m_\pi^2) + 4h_2m_\pi^2 \right](l\cdot q\epsilon_\psi^\lambda - q\cdot\epsilon_\psi l^\lambda) \right. \\ &\quad + \frac{1}{2}h_3[-l_\alpha q\cdot\epsilon_\psi(k_+^\lambda k_+^\alpha - k_-^\lambda k_-^\alpha) \\ &\quad + \epsilon_\psi^\lambda l_\alpha q_\beta(k_+^\alpha k_+^\beta - k_-^\alpha k_-^\beta) \\ &\quad - l^\lambda q_\alpha\epsilon_{\psi\beta}(k_+^\alpha k_+^\beta - k_-^\alpha k_-^\beta) \\ &\quad \left. + l\cdot q\epsilon_{\psi\alpha}(k_+^\lambda k_+^\alpha - k_-^\lambda k_-^\alpha)] \right\}, \end{aligned} \tag{12}$$

where α,β,λ are Lorentz indices and $D_X(q^2)$ is the denominator of the $X(4260)$ propagator, which will be discussed later.

Following the helicity amplitude decomposition method [41] and choosing the basis of tensors

$$\begin{aligned} \tilde{t}^{(0)} &= 1, \\ \tilde{t}^{(1)} &= k_-^\mu, \\ \tilde{t}^{(2)} &= k_-^\mu k_-^\nu - \frac{1}{3}k_-^2\tilde{g}^{\mu\nu}, \qquad \left(\tilde{g}^{\mu\nu} = g^{\mu\nu} - \frac{k_+^\mu k_+^\nu}{k_+^2}\right), \end{aligned} \tag{13}$$

it is easy to separate the S-wave and D-wave components of the $\pi\pi$ system. The overall S-wave amplitude reads

$$
\begin{aligned}
i\mathcal{A}_s^{\rm tree} = & \frac{i4eg_0}{M_{J/\psi}F_\pi^2 q^2 D_X(q^2)}\bar{v}(q_1,s)\gamma_\lambda u(q_2,s')\epsilon_{\psi\omega}\left\{\left[4h_1\frac{1}{2}(s-2m_\pi^2)+4h_2m_\pi^2\right](l\cdot q g^{\lambda\omega}-q^\omega l^\lambda)\right. \\
& +\frac{1}{2}h_3\left[-\frac{1}{3}\rho^2(s)l_\lambda q^\omega s+\left(1-\frac{1}{3}\rho^2(s)\right)k_+^\lambda q^\omega l\cdot k_+ +\frac{1}{3}\rho^2(s)l\cdot q g^{\lambda\omega}s\right. \\
& -\left(1-\frac{1}{3}\rho^2(s)\right)g^{\lambda\omega}k_+\cdot q k_+\cdot l-\frac{1}{3}\rho^2(s)l_\lambda q^\omega s+\left(1-\frac{1}{3}\rho^2(s)\right)k_+^\lambda l^\omega q\cdot k_+ \\
& \left.\left.+\frac{1}{3}\rho^2(s)l\cdot q g^{\lambda\omega}s-\left(1-\frac{1}{3}\rho^2(s)\right)k_+^\lambda k_+^\omega q\cdot l\right]\right\}, \qquad (14)
\end{aligned}
$$

whereas the D-wave part is

$$
\begin{aligned}
i\mathcal{A}_d^{\rm tree} = & \frac{i4eg_0}{M_{J/\psi}F_\pi^2 q^2 D_X(q^2)}\bar{v}(q_1,s)\gamma_\lambda u(q_2,s')\epsilon_\psi^\omega \\
& \times\frac{1}{2}h_3(t_2^{\lambda\alpha}l_\alpha q_\omega - t_2^{\alpha\beta}g_{\lambda\omega}l_\alpha q_\beta + t_2^{\alpha\beta}g_{\beta\omega}l_\lambda q_\alpha \\
& - t_2^{\lambda\alpha}g_{\alpha\omega}l\cdot q) \\
\equiv & \frac{2eg_0h_3}{F_\pi^2 M_{J/\psi}q^2 D_X(q^2)}B_d. \qquad (15)
\end{aligned}
$$

The standard Breit-Wigner type of $X(4260)$ propagator is parametrized as $D_X(q^2)=M_X^2-q^2-iM_X\Gamma_X(q^2)$, where $\Gamma_X(q^2)$ is the total decay width including the partial widths of all possible channels, which will be discussed later.

Since the D-wave contribution is proportional to the fourth power of the kinematic factor $\rho(s)$, it is highly suppressed compared with the S-wave contribution. Through numerical studies it is shown that the D-wave contribution is roughly less than 1% of the total decay rate, and therefore we will not include it in the fitting process in this work.

C. Final-state interactions

The tree-level amplitude as described in Sec. II B is not sufficient to describe the $X\to J/\psi\pi\pi$ decay process, since the $\pi\pi$ system undergoes strong final-state interactions, especially in the $IJ=00$ channel. To include FSI, the following decay amplitude is proposed [42]:

$$
\begin{aligned}
\mathcal{A}_1 &= \mathcal{A}_1^{\rm tree}\alpha_1(s)\mathcal{T}_{11}(s)+\mathcal{A}_2^{\rm tree}\alpha_2(s)\mathcal{T}_{21}(s), \\
\mathcal{A}_2 &= \mathcal{A}_1^{\rm tree}\alpha_1(s)\mathcal{T}_{12}(s)+\mathcal{A}_2^{\rm tree}\alpha_2(s)\mathcal{T}_{22}(s), \qquad (16)
\end{aligned}
$$

where the subscripts 1 and 2 denote the $\pi\pi$ and $K\bar{K}$ final states, respectively; $\mathcal{T}_{11}$, $\mathcal{T}_{12}$, and $\mathcal{T}_{22}$ are unitarized partial wave amplitudes representing $\pi\pi\to\pi\pi$, $\pi\pi\to K\bar{K}$, and $K\bar{K}\to K\bar{K}$ scatterings, respectively. They are constructed from the one-loop chiral perturbative amplitude

$$
T\equiv\begin{pmatrix} T_{11}, & T_{12} \\ T_{21}, & T_{22}\end{pmatrix}
$$

using the [1, 1] Padé approximation,

$$
\mathcal{T}=T^{(2)}\frac{1}{T^{(2)}-T^{(4)}}T^{(2)}, \qquad (17)
$$

where the superscripts (2) and (4) represent $O(p^2)$ and $O(p^4)$ chiral amplitudes, respectively. In such a way, the scattering matrix $\mathcal{T}$ is unitary ($\mathcal{T}_{21}=\mathcal{T}_{12}$),

$$
\begin{aligned}
{\rm Im}\mathcal{T}_{11} &= \mathcal{T}_{11}^*\rho_1 T_{11}+\mathcal{T}_{12}^*\rho_2 T_{21}, \\
{\rm Im}\mathcal{T}_{12} &= \mathcal{T}_{12}^*\rho_2 T_{22}+\mathcal{T}_{11}^*\rho_1 T_{12}, \\
{\rm Im}\mathcal{T}_{22} &= \mathcal{T}_{21}^*\rho_1 T_{12}+\mathcal{T}_{22}^*\rho_2 T_{22}. \qquad (18)
\end{aligned}
$$

In Eq. (16) the functions α_i are mild polynomials which play the role of offsetting the "left-hand" cuts on the complex s plane in the amplitude $\mathcal{T}$ that should not appear in the function $\mathcal{A}$. The unitarity relations of Eq. (16) are then automatically satisfied. Further, in $\alpha_1(s)$ an additional pole term is added:

$$
\alpha_1(s)=\frac{c_0^{(1)}}{s-s_A}+c_1^{(1)}+c_2^{(1)}s+\cdots, \qquad (19)
$$

where s_A represents the Adler zero of T_{11}. The role of the pole term is to cancel the Adler zero that is hidden in T_{11} but not welcome in A [42].[1] Up to the leading order in chiral perturbation theory, one finds $c_0^{(1)}=16\pi F_\pi^2$ and $s_A=m_\pi^2/2$ in the $I=0$ S-wave. However in the [1, 1] matrix Padé amplitude, $s_A=(0.490-0.008i)m_\pi^2$ and we fix $c_0^{(1)}=(0.330-0.001i)\ {\rm GeV}^2=(0.779-0.002i)16\pi F_\pi^2$.[2]

In V1, three different representations of the T matrices were used for the fit (the coupled-channel Padé approximation [43], K-matrix unitarization [44], and the Peking

[1] An advantage of the pole term in Eq. (19) is that, by appropriately choosing the coefficient $c_0^{(1)}$ as $\lim_{s\to s_A}\frac{c_0^{(1)}}{s-s_A}\times T_{11}(s)=1$, it guarantees $\mathcal{A}_1=\mathcal{A}_1^{\rm tree}+O(s^2)$.

[2] The Adler zero moves to the complex plane because the existence of the left-hand cut $(-\infty,4m_K^2-4m_\pi^2]$ of T_{22}, which has been taken into T_{11} due to the matrix Padé approximation (and similarly for that of c_0^1.)

TABLE I. Low-energy constants from the coupled-channel Padé amplitudes. Here these parameters are refitted and are slightly different from those in Ref. [43]. The unit is 10^{-3}.

L_1	L_2	L_3	L_4	L_5	$2L_6+L_8$	$2L_7+L_8$
0.881	1.029	−3.803	0.176	1.111	1.123	0.392

University Representation (PKU) [45]); however, not much difference was obtained. Therefore, we only keep the Padé amplitude in this work to perform the fit to the $\pi\pi$ invariant mass spectrum. In Table I we list the low-energy constants of the $O(p^4)$ chiral Lagrangian being used here.[3] For more details about these T matrices, we refer to the original literature.

III. NUMERICAL ANALYSIS

A. The experimental data and fit process

Once the $X(4260)\to J/\psi\pi\pi$ amplitude is calculated from Eq. (16), one obtains the decay width $\Gamma_{J/\psi\pi\pi}$, the cross section $e^+e^-\to X(4260)\to J/\psi\pi\pi$, and the $\pi\pi$ invariant mass spectrum. In this subsection we focus on how to write down the correct form of the denominator for the $X(4260)$ propagator.

Beside the $J/\psi\pi\pi$ channel indicated by the experiment, the $X(4260)$ may also decay into $h_c\pi\pi$, and there are other nearby thresholds close to $X(4260)$, such as $\chi_{c0}\omega$ (4197 MeV), $D_s^{*+}\bar{D}_s^{*-}$ (4224 MeV), $D^-D_1^+(2420)$ (4291 MeV), $\chi_{c1}\omega$ (4293 MeV), etc. It is possible that $X(4260)$ couples to all of these channels. Therefore a careful method is to write down the denominator of the $X(4260)$ propagator as

$$D_X(q^2)=M_X^2-q^2-i\sqrt{q^2}\Gamma(q^2), \tag{20}$$

where $\Gamma_X(q^2)$ consists of all partial widths,

$$\Gamma_X(q^2)=\Gamma_{J/\psi\pi\pi}(q^2)+\Gamma_{h_c\pi\pi}+g_{\omega\chi_{c0}}k_{\omega\chi_{c0}}+g_{D_s^*D_s^*}k^3_{D_s^*D_s^*}+g_{DD_1}k_{DD_1}+g_{\omega\chi_{c1}}k_{\omega\chi_{c1}}+\Gamma_0. \tag{21}$$

Here $\Gamma_{J/\psi\pi\pi}(q^2)$ is calculated from the above amplitude of $X(4260)\to J/\psi\pi\pi$, and $k_{\omega\chi_{c0}}$, $k_{D_s^*D_s^*}$, k_{DD_1}, and $k_{\omega\chi_{c1}}$ are the 3-momentum of $\omega\chi_{c0}$, $D_s^*D_s^*$, DD_1, and $\omega\chi_{c1}$ in the $X(4260)$ rest frame, respectively. The $D_s^*D_s^*$ channel begins with a P-wave coupling, and therefore it depends on the third-order momentum, and the other three channels are of S-wave couplings and hence only depend on their first-order momentum. The possible rest partial widths are parametrized as a constant Γ_0. For $h_c\pi\pi$, since the channel momentum $k_{h_c\pi\pi}$ behaves like a constant near $q^2=M_X^2$, we parametrize $\Gamma_{h_c\pi\pi}$ as a constant too. Notice that $\Gamma_{h_c\pi\pi}/\Gamma_{J/\psi\pi\pi}(M_X^2)$ is constrained by experiment. We discuss this point in more detail in the next section.

One may notice that $Z_c\pi$ is also a possible decay channel of $X(4260)$ but it is not considered in this work, since the contribution of $X(4260)\to Z_c\pi\to J/\psi\pi\pi$ can be absorbed into the $XJ/\psi\pi\pi$ contact interaction in the Lagrangian (6). To confirm this viewpoint, we tested the contribution of $Z_c\pi$ with the Breit-Wigner parametrization of Z_c, and found that there was not much difference between the $J/\psi\pi\pi$ and $\pi\pi$ spectra with and without its contribution. Therefore we exclude the $Z_c\pi$ contribution in this paper and leave it for future work.

In the present work we fit the $X(4260)$ line shape in the region 4.15 GeV$<\sqrt{q^2}<$ 4.47 GeV, where the data is from Ref. [3] (16 data points) and Ref. [5] (16 data points); see in Fig. 5(a). The total cross section of $e^+e^-\to J/\psi\pi\pi$ is given by

$$\sigma_{e^+e^-\to J/\psi\pi^+\pi^-}=\int_{s_-}^{s_+}\int_{t_-}^{t_+}\frac{\overline{|\mathcal{A}_1|}^2 dsdt}{(2\pi)^3 32(q^2)^2}, \tag{22}$$

where $t=(q-q^-)^2$, $\mathcal{A}_1$ is defined in Eq. (16) and the lower and upper limits are given as

$$\begin{aligned}
s_- &= 4m_\pi^2,\\
s_+ &= \left(\sqrt{q^2}-M_\Psi\right)^2,\\
t_\pm &= \frac{1}{4s}\{(q^2-M_\Psi^2)^2\\
&\quad -[\lambda^{1/2}(q^2,s,M_\Psi^2)\mp\lambda^{1/2}(s,m_\pi^2,m_\pi^2)]^2\},\\
\lambda(a,b,c) &= (a-b-c)^2-4bc.
\end{aligned} \tag{23}$$

With Eq. (23), one finds that for a larger q^2 the upper limit of s becomes too large to ensure the validity of the parametrization introduced in Sec. II C.[4] For the $\pi\pi$ invariant mass spectrum we use the data given in Fig. 4b of Ref. [3], corresponding to $\sqrt{q^2}\in[4.2,4.4]$ GeV (17 data points), the data $\sqrt{q^2}\in[4.15,4.45]$ GeV (41 data points) in Ref. [5], and the data $\sqrt{q^2}$ fixed at 4.26 GeV (44 points) from the recent experiment reported in Ref. [29]. For the first set of data, a Monte Carlo study of the efficiency correction at $\sqrt{q^2}=4.26$ GeV was performed in Ref. [3], and through a numerical test we find that the

[3]We noticed that for these low energy constant (LECs) there is a difference between ours [43] (L_i^O) and that in the earlier work [46] (L_i^P): $L_i^P=L_i^O+\frac{\Gamma_i}{32\pi^2}$. This is because we calculated in the $\overline{\text{MS}}$ scheme and theirs was calculated in the $\overline{\text{MS}}-1$ scheme. To compare with their work we need to transform our LECs into L_i^P, which was performed incorrectly in Ref. [43]; we correct it here.

[4]For $\sqrt{q^2}=4.47$ GeV, it corresponds to a value $\sqrt{s}\simeq 1.17$ GeV which is within the range where T can provide a reasonable description.

efficiency curve is well reproduced by the $\pi\pi$ two-body phase space up to a normalization constant; hence, in our fit we simply use the two-body phase space instead of the efficiency-corrected one. We assume the other two sets of data maintain similar behavior. In total, there are 145 data points in the $\pi^+\pi^-$ invariant mass spectrum to be used.

Recently, the cross section of the $\omega\chi_{c0}$ channel was measured in the range [4.21, 4.45] GeV [36,37], where a rough structure of the $X(4260)$ could be observed at 4.26 GeV. If we assume the events in Refs. [36,37] all came from $X(4260)$ decay, then nine data points can be used. Nevertheless, it may be possible that these events come from the continuum rather than from $X(4260)$; hence, in our fit we carefully consider this possibility. That is, in the following section, the fit named Fit I does not include the $\omega\chi_{c0}$ cross section data, while in Sec. III C the $\omega\chi_{c0}$ cross section data are fitted, which we call Fit II. It is found that Fit I does not differ much from the result of V1 (notice that here we include the $h_c\pi\pi$ channel), but Fit II, which includes the $\omega\chi_{c0}$ data, violates the approximate "scaling law" found in V1 and leads to a small value of $\Gamma_{e^+e^-}$.

The parameters needed in our fit are the following. First, Eqs. (4) and (6) describing the γ—X transition and the tree-level $X(4260)$ J/ψ $\pi\pi(K\bar{K})$ interactions provide four parameters. Second, it is found that taking $\alpha_{1,2}(s)$ to be linear polynomials (except the Adler zero term) is already good enough for data fitting, and hence the two $\alpha_i(s)$ [$i = 1, 2$ and each $\alpha_i(s)$ contains two parameters] contribute another four parameters. Third, the mass M_X of the $X(4260)$ in the propagator and the coupling constant $g_{\omega\chi_{c0}}$ bring another two parameters. Finally, there are three normalization factors N_1, N_2, and N_3 for the $\pi^+\pi^-$ invariant mass spectra of Belle, *BABAR*, and BESIII, respectively. After summing up there are 13 total parameters.

We also studied the parameters $g_{D_s^*D_s^*}$, g_{DD_1}, $g_{\omega\chi_{c1}}$, and Γ_0 through rather extensive numerical tests in different environments, and we found that $g_{D_s^*D_s^*}$, g_{DD_1}, and $g_{\omega\chi_{c1}}$ are always vanishingly small, which suggests that the coupling of $X(4260)$ to $D_s^*D_s^*$, $DD_1(2420)$, and $\omega\chi_{c1}$ are negligible, compared to $J/\pi\pi$, $\omega\chi_{c0}$ and $h_c\pi\pi$. Moreover, the parameter Γ_0 tends to vanish in all of the different fits and hence it can be ignored too.[5] Therefore we will not include the couplings to $D_s^*D_s^*$, $DD_1(2420)$, $\omega\chi_{c1}$, and Γ_0 in our discussion from now on.

B. Fit without $\omega\chi_{c0}$ data

In this fit, which we call Fit I, only the $J/\psi\pi\pi$ cross section and $\pi\pi$ invariant mass spectrum are included, and not the $\omega\chi_{c0}$ cross section data, which will be analyzed in the next section. Regarding the $h_c\pi\pi$ channel, however, on the one hand the rough shape due to the lack of precision is not an appropriate to fit. [47] On the other hand, it is not clear yet whether they are from the $X(4260)$ resonance or from the continuous background. As pointed out in Ref. [28], $h_c\pi\pi$ is a suppressed decay mode of $X(4260)$ compared with $J/\psi\pi\pi$ because the heavy-quark spin flip violates heavy-quark symmetry. Therefore, we assume that $h_c\pi\pi$ has an unknown width in the $X(4260)$ propagator; it is assumed to be a constant because its threshold is far away from the $X(4260)$ resonance,[6] and it is constrained by the width of $\Gamma_{J/\psi\pi\pi}(q^2)$ by the following relation:

$$\Gamma_{h_c\pi\pi} = R \times \Gamma_{J/\psi\pi\pi}(q^2)|_{q=4.26\ \mathrm{GeV}}, \tag{26}$$

where the coefficient $R = 0.66$ is a rough estimation from the ratio of $\sigma_{h_c\pi\pi}/\sigma_{J/\psi\pi\pi}$ at $q = 4.26$ GeV [38]. Of course, we will also test the fits with different R values ranging from 0 to 0.66.

When fit to the $J/\psi\pi\pi$ cross section and the $\pi\pi$ invariant mass, we found that the value of g_0 has a large uncertainty.

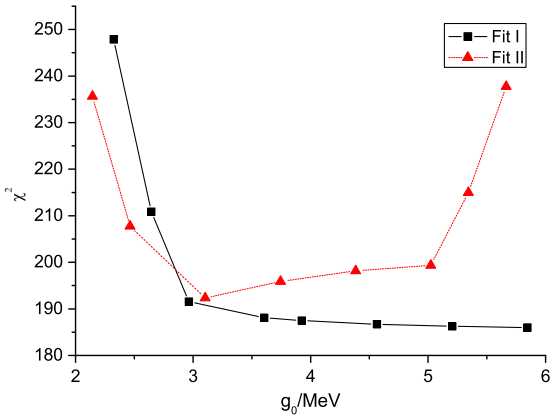

FIG. 4 (color online). χ^2 dependence on g_0. Fit I is without the $\omega\chi_{c0}$ data, where we see the scaling behavior, whereas Fit II is with the $\omega\chi_{c0}$ data, where the scaling behavior disappears.

[5]It is exactly for this reason that we will band the $h_c\pi\pi$ width with the $J/\Psi\pi\pi$ width with a ratio R [see Eq. (26)]; otherwise, the fit program will tend to destroy it.

[6]In fact, the momentum-dependent width of the $h_c\pi\pi$ channel with a form factor is also tested in the fitting as follows:

$$\Gamma_{h_c\pi\pi}(q^2) \sim \int \frac{\sqrt{(q^2-(\sqrt{s}+m_{h_c})^2)(q^2-(\sqrt{s}-m_{h_c})^2)}\sqrt{s-4m_\pi^2}}{4qs} \times ds d\Omega, \tag{24}$$

and

$$\Gamma_X(q^2) = (\Gamma_{J/\psi\pi\pi}(q^2) + \Gamma_{h_c\pi\pi}(q^2)) \exp\left(\frac{q^2-M_X^2}{\Lambda^2}\right) + g_{\omega\chi_{c0}} k_{\omega\chi_{c0}} + \cdots. \tag{25}$$

This fitting result is always similar to the constant width of $h_c\pi\pi$, and therefore only the constant $\Gamma_{h_c\pi\pi}$ is shown in the text.

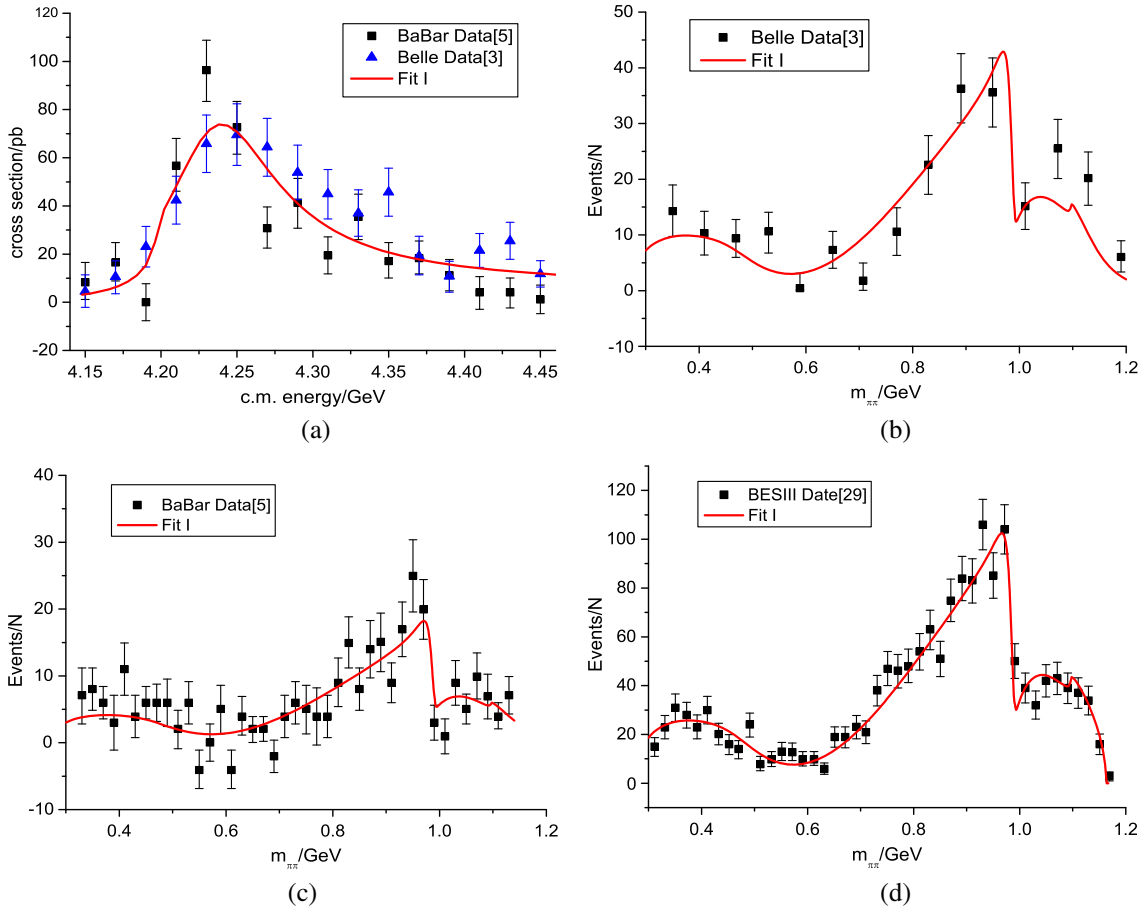

FIG. 5 (color online). The fit to the cross section $e^+e^- \to J/\psi\pi\pi$ and $\pi\pi$ invariant mass spectrum without $\omega\chi_{c0}$ data. (a) Fit to $J/\psi\pi\pi$ cross section data of Refs. [3,5]. (b) Fit to $\pi\pi$ invariant mass spectrum of Ref. [3]. (c) Fit to $\pi\pi$ invariant mass spectrum of Ref. [5]. (d) Fit to $\pi\pi$ invariant mass spectrum of Ref. [29].

Since it characterizes the transition between $X(4260)$ and the photon field, or $\Gamma_{X\to e^+e^-}$ according to Eq. (5), it should not be too large to avoid the upper bound established by an analysis of the BES experiment: Ref. [48] gives $\Gamma_{X\to e^+e^-} < 420$ eV, or most conservatively <580 eV, at the 90% confidence level. The dependence of χ^2 on g_0 is clearly depicted in Fig. 4 (black squares), which exhibits an approximate scaling law of the parameter g_0. When g_0 increases, the parameters h_i have to become small to compensate for the experimental value of $\Gamma_{X\to J/\Psi\pi\pi}$ as given in Eq. (6). Looking at Eqs. (4) and (14), it is easy to see out that $\Gamma_{X\to J/\Psi\pi\pi}$ is proportional to the product of g_0 and h_i. This mechanism keeps $\Gamma(q^2)$ in the denominator of the $X(4260)$ propagator [see Eq. (20)] almost unchanged when g_0 varies. As a consequence, χ^2 becomes almost inert with respect to the variation of g_0 when it is large enough, since the effect can be counterbalanced by a variation of h_i. This observation was already made in V1; here, we reconfirm the "scaling law" even when $\Gamma_{h_c\pi\pi}$ is included.

The "scaling law" means that we cannot reliably determine the parameter g_0 at all when g_0 is large enough. It is important to notice that in Fig. 4 there exists a large enough space for g_0 to maintain a (almost) minimal χ^2, and at lower values it is below the BES $\Gamma_{X\to e^+e^-}$ bound given in Ref. [48]. As an example, we list the lowest value of g_0 at 4.24 MeV which corresponds to $\Gamma_{X\to e^+e^-} \simeq 41.1$ eV, and its fitting result is shown in Fig. 5 and Table II. For this

TABLE II. Parameters from Fit I and Fit II. The ratio R is chosen as 0.66, for example. Since g_0 is fixed, the total number parameters is 12, and only the important parameters are presented.

	Fit I	Fit II
χ^2/d.o.f.	187.1/(145-12)	193.5/(154-13)
g_0 (MeV)	4.24 (fixed)	3.32 ± 0.11
$g_{Y\omega\chi_{c0}}$	0.17 ± 0.01	0.06 ± 0.01
M_X (GeV)	4.2504 ± 0.0034	4.2432 ± 0.0031

TABLE III. Definition of the four Riemann sheets with the $J/\psi\pi\pi$ ($h_c\pi\pi$) channel and $\omega\chi_{c0}$ channel.

	Sheet I	Sheet II	Sheet III	Sheet IV
$\Gamma_{J/\psi\pi\pi} + \Gamma_{h_c\pi\pi}$	+	−	−	+
$\Gamma_{\omega\chi_{c0}}$	+	+	−	−

TABLE IV. Pole position of Fits I and II. The value of $\sqrt{s_{\rm pole}} = M_{\rm pole} - i\Gamma_{\rm pole}/2$ is given in MeV.

	Sheet I	Sheet II	Sheet III	Sheet IV
Fit I	–	–	4231.9-44.2i	4233.2-42.5i
Fit II	–	4241.5-24.4i	4232.8-36.3i	–

chosen value, Table II indicates that the widths of $J/\psi\pi\pi$, $h_c\pi\pi$, and $\omega\chi_{c0}$ at $\sqrt{q^2} = 4.26$ GeV are 32.4, 21.3, and 49.8 MeV, respectively.

We also search for poles of the $X(4260)$ propagator; the complex plane is divided into four Riemann sheets by $\Gamma_{J/\psi\pi\pi}$ ($\Gamma_{h_c\pi\pi}$) and $\Gamma_{\omega\chi_{c0}}$ defined in Table III, and the pole positions are presented in Table IV. It is noticeable that there are two

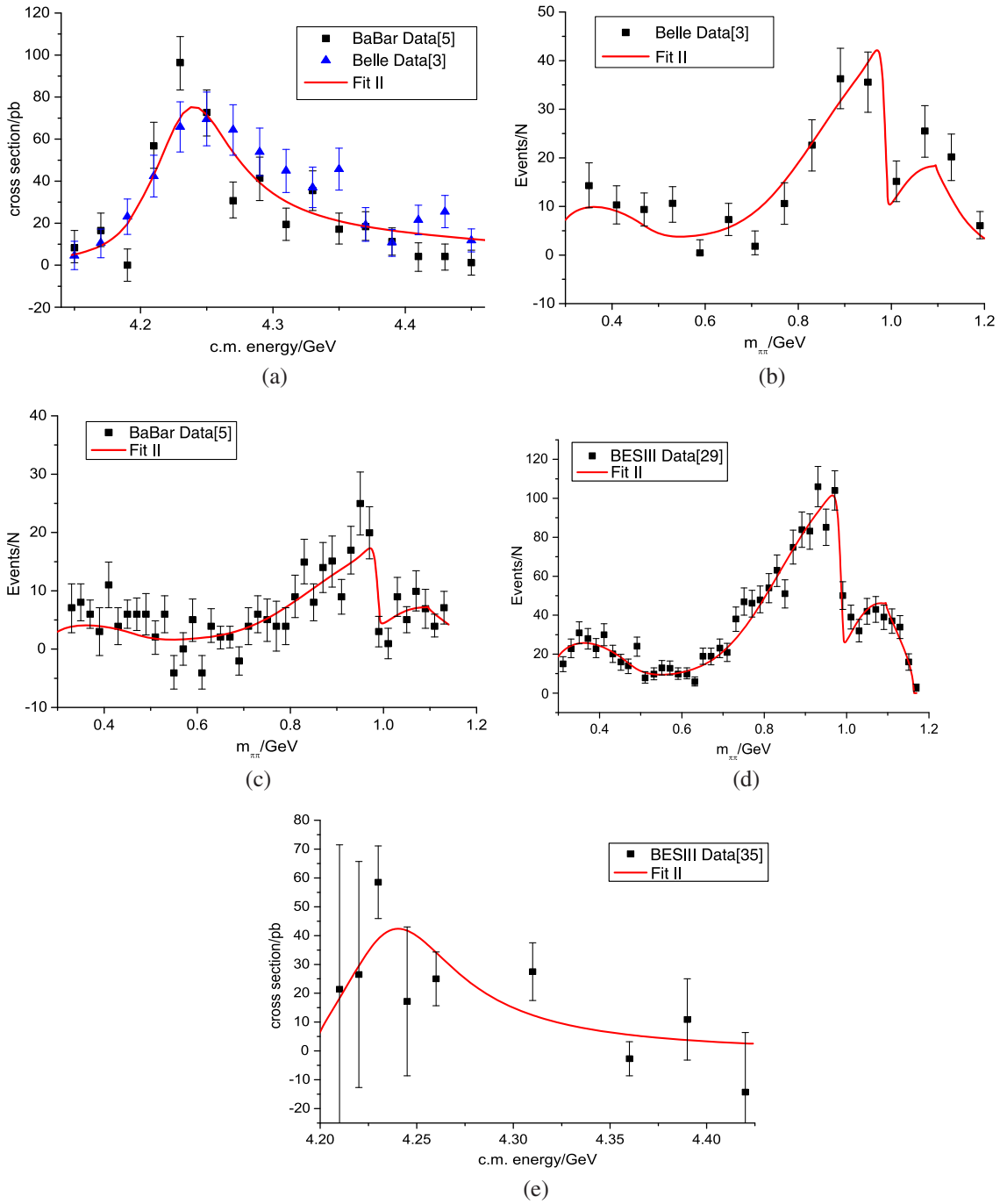

FIG. 6 (color online). The cross section of $e^+e^- \to J/\psi\pi\pi$, the invariant mass of $\pi\pi$, and the cross section of $e^+e^- \to \omega\chi_{c0}$. (a) Fit to $J/\psi\pi\pi$ cross section data of Refs. [3,5]. (b) Fit to $\pi\pi$ invariant mass spectrum of Ref. [3]. (c) Fit to $\pi\pi$ invariant mass spectrum of Ref. [5]. (d) Fit to $\pi\pi$ invariant mass spectrum of Ref. [29]. (e) Fit to $\omega\chi_{c0}$ cross section data of Ref. [35].

pairs of poles located above the $\omega\chi_{c0}$ threshold on the third and fourth sheets, and both of them show a roughly 85 MeV pole width for the $X(4260)$ resonance. According to the pole-counting rule in Refs. [49,50], the two pairs of near-threshold poles indicate that $X(4260)$ is not like a molecule resonance, but rather more like an "elementary" particle or (in other words) a confining state.

For the purpose of extracting solid physical conclusions, we also vary the coefficient R as 0.56,0.46,0.36,0.26,0.16,0 in the fit, and when $R = 0$ the fit procedure is very similar to that in V1 [35], where we found a large coupling constant $g_{\omega\chi_{c0}}$ and also the χ^2 scaling law on g_0. It is found that qualitative physical results are not sensitive to the R value, and all the fits with different R values maintain the same scaling law of the coupling constant g_0. In all cases the large coupling of the $\omega\chi_{c0}$ to $X(4260)$ always exists, which coincides with the prediction in V1.

Before going to the next section, a brief conclusion is in order: the fit result shows that the χ^2 has an approximate scaling law of g_0, which could not be determined very well. Two nearby poles are found on the third and fourth Riemann sheets. The fit results are not sensitive to the R value, which indicates that $h_c\pi\pi$ only contributes to $X(4260)$ decay as a smooth background. We predict that the $\omega\chi_{c0}$ channel has a large branching ratio in $X(4260)$ decay in all cases.

C. Fit including $\omega\chi_{c0}$ cross section data

In the previous subsection, we confirmed that there should be a sizable contribution from the $\omega\chi_{c0}$ channel even when the recent $\omega\chi_{c0}$ cross section data from the BESIII Collaboration [36,37] are not taken into consideration. In this subsection, we include the $\omega\chi_{c0}$ cross section data in our analysis to get a more precise result for $g_{\omega\chi_{c0}}$. This will certainly benefit our understanding of $X(4260)$, provided that the $\omega\chi_{c0}$ data indeed come from $X(4260)$ decay. The cross section of $e^+e^- \to X(4260) \to \omega\chi_{c0}$ is parametrized as in Ref. [4],

$$\sigma_{e^+e^-\to X(4260)\to\omega\chi_{c0}}(q^2) = \frac{3\pi}{4q^2}\frac{\Gamma_{ee}\Gamma_{\omega\chi_{c0}}}{|D_X(q^2)|^2}, \qquad (27)$$

where Γ_{ee} is given in Eq. (5), $D_X(q^2)$ is the denominator of the $X(4260)$ propagator shown in Eqs. (20) and (21), and $\Gamma_{\omega\chi_{c0}} = g_{\omega\chi_{c0}}k_{\omega\chi_{c0}}$.

The major difference after including the $\omega\chi_{c0}$ data in Fit II is that the χ^2 scaling law of g_0 disappears. As shown in Fig. 4 (green triangles), the χ^2 has a minimum at $g_0 \simeq 3.32$ MeV. This suggests that this fit is more stable than Fit I without the $\omega\chi_{c0}$ cross section.

We again take $R = 0.66$ as an example: the fit result is shown in Fig. 6 and Table II. From Table II, one notices that the coupling of $\omega\chi_{c0}$ approaches a smaller value (but still much larger than other open-charm channels), which is well constrained by the new data of $X(4260)$ decaying into $\omega\chi_{c0}$. The pole positions are also searched for and are shown in Table IV. It should be noticed that there are two pairs of poles on sheets II and III, which has a smaller pole width (around 60 MeV) compared to Fit I.

TABLE V. Partial widths obtained when R changes. Γ_{ee} is in units of eV and the others are in units of MeV.

	Fit II						
R	0.66	0.56	0.46	0.36	0.26	0.16	0.00
Γ_{ee}	25.23	24.36	23.55	22.82	22.19	22.03	22.02
$\Gamma_{\omega\chi_{c0}}$	17.49	19.04	20.89	23.11	25.84	26.75	26.77
$\Gamma_{J/\psi\pi\pi}$	54.52	57.02	59.67	62.42	65.21	65.82	65.02
$\Gamma_{h_c\pi\pi}$	35.99	31.93	27.45	22.47	16.95	10.53	0

Comparing the χ^2/d.o.f., Fit II (193.5/141) is similar in quality to Fit I (187.1/133). The greatest physical difference once the $\omega\chi_{c0}$ data are included is that it roughly reduces $g_{\omega\chi_{c0}}$ by a factor of 3. The three partial widths $\Gamma_{J/\psi\pi\pi}$, $\Gamma_{h_c\pi\pi}$, and $\Gamma_{\omega\chi_{c0}}$ are now 45.1, 29.9, and 16.9 MeV at $\sqrt{q^2} = 4.26$ GeV, respectively. The branching ratio of $\omega\chi_{c0}$ in this fit is 18.5%, which is still sizable, and it is still much larger compared with open-charm channels, such as $D\bar{D}$, $D^*\bar{D}^*$, and $D_s^*\bar{D}_s^*$. Furthermore, we verified that the qualitative result is not sensitive to the ratio R in the range [0, 0.66] (see Table V for an illustration).

In summary, after taking the $\omega\chi_{c0}$ cross section data into account, the coupling of $X(4260)$ decay into $\omega\chi_{c0}$ becomes smaller but fixable; even though it is no longer dominant, it still plays an important role in $X(4260)$ decay, which supports our previous conclusion. Certainly, because of the large error bar near 4.26 GeV from the $\omega\chi_{c0}$ cross section data [in Fig. 6(e)], a more qualitative conclusion would still need more statistics from the experimental data.

IV. CONCLUSIONS AND DISCUSSION

Despite being discovered almost ten years ago, the properties of $X(4260)$ remain mysterious. The nature of this particle is still a controversial issue. In this work, we investigated this particle based on all experimental data available and very modest theoretical assumptions. Hence, the conclusion we reached should be robust. Compared with V1 [35], two more channels—$h_c\pi\pi$ and $\omega\chi_{c0}$—were considered.

We have performed two fits: one without (Fit I) and one with (Fit II) the $\omega\chi_{c0}$ cross section data. The two scenarios have similar χ^2/d.o.f. but different behavior for the coupling constant g_0. In the former, a χ^2 scaling law of g_0 is observed which could not be determined from the fit, while in the latter case the χ^2 scaling law of g_0 disappears, which has a minimum value when $g_0 = 3.32$ MeV. The value of g_0 corresponds to $\Gamma_{e^+e^-} \simeq 25$ eV, which is certainly below the $\Gamma_{e^+e^-}$ bound from the BES experiment [48]. Considering the variation of R, we also give the following estimate:

$$\Gamma_{ee} = 23.30 \pm 3.55 \text{ eV}. \quad (28)$$

Compared with the experimental observation of $\Gamma_{ee} \times \mathrm{Br}(J/\psi\pi\pi) = 9.7 \pm 1.1$ eV [3] or 9.2 ± 1.5 eV [5], we conclude that the branching ratio of X(4260) decay into $J/\psi\pi\pi$ is roughly 0.5. Finally, our analysis points out a sizable coupling between $X(4260)$ and $\omega\chi_{c0}$. From the viewpoint of heavy-quark symmetry, since $\omega(1^{--})\chi_{c0}(0^{++})$ also conserves heavy-quark spin it is natural to expect that its partial width is similar than that of $J/\psi\pi\pi$.[7]

Although our result is still rather far from reaching any sound conclusion about the nature of $X(4260)$, some useful information may be drawn from our analysis. In both Fits I and II there are two nearby poles found in the $X(4260)$ propagator, indicating that $X(4260)$ is most likely a confining state [49,50]. This conclusion disfavors the molecular interpretation of $X(4260)$. Nevertheless, one has to be cautious in making a quick conclusion: the pole-counting rule [49] is based upon nonrelativistic quantum scattering theory, and hence it may not be valid for a molecular bound state made of one heavy and one light particle [19].

The small value of $\Gamma_{e^+e^-}$ may be consistent with the hybrid scenario which indicates 5.5 ± 1.3 eV $\leq \Gamma_{e^+e^-} \leq 62 \pm 15$ eV [10] or 23 ± 20 eV [14]. Also the hybrid state is suppressed to decay into $D\bar{D}$, $D_s\bar{D}_s$, $D^*\bar{D}^*$, and $D_s^*\bar{D}_s^*$ [51], which coincides with the experimental data for $X(4260)$. Nevertheless, since D_1 is in the P wave, a hybrid state is likely to have a large coupling to the DD_1 channel; this is not supported by experiment [52] or our analysis. It should be pointed out that a small value of $\Gamma_{e^+e^-}$ is also consistent with the explanation that $X(4260)$ is the 3D charmonium state. The difficulty of this possible explanation comes from the role of $X(4160)$, which is considered as a candidate for the 3D charmonium state in the literature, though it has a rather large $\Gamma_{e^+e^-}$ width.

The analysis made in this paper suggests that $X(4260)$ is a confining state rather than a molecular bound state. Therefore, a tetraquark state can also be a possible explanation for $X(4260)$. $X(3872)$ is also a confining state [50] and the former may hence be considered as the 1^{--} counterpart of the latter [28]. The major difficulty for the tetraquark scenario was also discussed in Ref. [28].

We hope our effort made in this paper will be helpful for clarifying the issue of $X(4260)$ in future investigations.

ACKNOWLEDGMENTS

We are grateful to illuminating discussions with Chang-Zheng Yuan and Kuang-Ta Chao, and we would also like to thank Gui-Jun Ding, Ce Meng, Qiang Zhao, and Bing-Song Zou for helpful discussions. This work is supported in part by the National Natural Science Foundation of China under contract numbers 10925522 and 11021092.

[7]The authors would like to thank one referee for illuminating this point.

[1] B. Aubert *et al.* (*BABAR* Collaboration), Phys. Rev. Lett. **95**, 142001 (2005).
[2] T. E. Coan *et al.* (CLEO Collaboration), Phys. Rev. Lett. **96**, 162003 (2006).
[3] C. Z. Yuan *et al.* (Belle Collaboration), Phys. Rev. Lett. **99**, 182004 (2007).
[4] K. A. Oilve (Particle Data Group), Chin. Phys. C **38**, 090001 (2014).
[5] J. Lees *et al.* (*BABAR* Collaboration), Phys. Rev. D **86**, 051102 (2012).
[6] S. Godfrey and N. Isgur, Phys. Rev. D **32**, 189 (1985).
[7] E. S. Swanson, Phys. Rep. **429**, 243 (2006).
[8] X. Liu, X. Q. Zeng, and X. Q. Li, Phys. Rev. D **72**, 054023 (2005).
[9] C. Z. Yuan, P. Wang, and X. H. Mo, Phys. Lett. B **634**, 399 (2006).
[10] F. E. Close and N. Page, Phys. Lett. B **628**, 215 (2005).
[11] S. L. Zhu, Phys. Lett. B **625**, 212 (2005).
[12] F. Buisseret and V. Mathieu, Eur. Phys. J. A **29**, 343 (2006).
[13] E. Kou and O. Pene, Phys. Lett. B **631**, 164 (2005).
[14] Y. Chen *et al.*, *Proc. Sci.*, LATTICE2013 (2013) 251.
[15] C. F. Qiao, Phys. Lett. B **639**, 263 (2006).
[16] J. L. Rosner, Phys. Rev. D **74**, 076006 (2006).
[17] G. J. Ding, Phys. Rev. D **79**, 014001 (2009).
[18] Q. Wang, M. Cleven, F. K. Guo, C. Hanhart, U. G. Meißner, X. G. Wu, and Q. Zhao , Phys. Rev. D **89**, 034001 (2014).
[19] S. Dubynskiy and M. Voloshin, Phys. Lett. B **666**, 344 (2008).
[20] E. van Beveren, G. Rupp, and J. Segovia, Phys. Rev. Lett. **105**, 102001 (2010).
[21] D.-Y. Chen, J. He, and X. Liu, Phys. Rev. D **83**, 054021 (2011).
[22] R. Albuquerque, F. Fanomezana, S. Narison, and A. Rabemananjara, Nucl. Phys. B, Proc. Suppl. **234**, 158 (2013).
[23] L. Maiani, V. Riquer, R. Faccini, F. Piccinini, A. Pilloni, and A. D. Polosa, Phys. Rev. D **87**, 111102 (2013).
[24] J.-R. Zhang and M.-Q. Huang, Phys. Rev. D **83**, 036005 (2011).
[25] D. Ebert, R. Faustov, and V. Galkin, Eur. Phys. J. C **58**, 399 (2008).
[26] D. Ebert, R. Faustov, and V. Galkin, Phys. At. Nucl. **72**, 184 (2009).
[27] L. Maiani, F. Piccinini, A. Polosa, and V. Riquer, Phys. Rev. D **72**, 031502 (2005).

[28] L. Maiani, F. Piccinini, A. Polosa, and V. Riquer, Phys. Rev. D **89**, 114010 (2014).
[29] M. Ablikim *et al.* (BESIII Collaboration), Phys. Rev. Lett. **110**, 252001 (2013).
[30] Z. Liu *et al.* (Belle Collaboration), Phys. Rev. Lett. **110**, 252002 (2013).
[31] T. Xiao, S. Dobbs, A. Tomaradze, and K. K. Seth, Phys. Lett. B **727**, 366 (2013).
[32] B. Aubert *et al.* (*BABAR* Collaboration), Phys. Rev. D **79**, 092001 (2009).
[33] G. Pakhlova *et al.* (Belle Collaboration), Phys. Rev. D **77**, 011103 (2008).
[34] G. Pakhlova *et al.* (Belle Collaboration), Phys. Rev. Lett. **98**, 092001 (2007).
[35] L. Dai, M. Shi, G.-Y. Tang, and H. Zheng, arXiv:1206.6911v2.
[36] C.-P. Shen, in Proceedings of the Workshop on Exotic States, Rizhao, China, 2014 (to be published).
[37] M. Ablikim *et al.* (BESIII Collaboration), Phys. Rev. Lett. **114**, 092003 (2015).
[38] M. Ablikim *et al.* (BESIII Collaboration), Phys. Rev. Lett. **111**, 242001 (2013).
[39] G. Ecker, J. Gasser, A. Pich, and E. de Rafael, Nucl. Phys. **B321**, 311 (1989).
[40] G. Ecker, J. Gasser, H. Leutwyler, A. Pich, and E. de Rafael, Phys. Lett. B **223**, 425 (1989).
[41] S. U. Chung, Phys. Rev. D **48**, 1225 (1993).
[42] K. L. Au, D. Morgan, and M. R. Pennington, Phys. Rev. D **35**, 1633 (1987).
[43] L. Y. Dai, X. G. Wang, and H. Q. Zheng, Commun. Theor. Phys. **57**, 841 (2012).
[44] Y. Mao, X.-G. Wang, O. Zhang, H. Q. Zheng, and Z. Y. Zhou, Phys. Rev. D **79**, 116008 (2009).
[45] Z. Y. Zhou, G. Y. Qin, P. Zhang, Z. G. Xiao, H. Q. Zheng, and N. Wu, J. High Energy Phys. 02 (2005) 043.
[46] A. G. Nicola and J. R. Pelaez, Phys. Rev. D **65**, 054009 (2002).
[47] C.-Z. Yuan, Chin. Phys. C **38**, 043001 (2014).
[48] X. H. Mo, G. Li, C Z. Yuan, K. L. He, H. M. Hu, J. H. Hu, P. Wang, and Z. Y. Wang, Phys. Lett. B **640**, 182 (2006).
[49] D. Morgan, Nucl. Phys. **A543**, 632 (1992).
[50] O. Zhang, C. Meng, and H. Q. Zheng, Phys. Lett. B **680**, 453 (2009).
[51] P. R. Page, E. S. Swanson, and A. P. Szczepaniak, Phys. Rev. D **59**, 034016 (1999).
[52] M. Ablikim *et al.* (BESIII Collaboration), Phys. Rev. Lett. **112**, 022001 (2014).